2018

Amino acid uptake measured by [18F]AFETP increases in response to arginine starvation in ASS1-deficient sarcomas

Bethany Cheree Prudner
Washington University School of Medicine in St. Louis

Fangdi Sun
Washington University School of Medicine in St. Louis

Jeffrey Charles Kremer
Washington University School of Medicine in St. Louis

Jinbin Xu
Washington University School of Medicine in St. Louis

Chaofeng Huang
Washington University School of Medicine in St. Louis

See next page for additional authors

IVYSPRING INTERNATIONAL PUBLISHER

Theranostics

2018; 8(8): 2107-2116. doi: 10.7150/thno.22083

Research Paper

Amino Acid Uptake Measured by [^{18}F]AFETP Increases in Response to Arginine Starvation in ASS1-Deficient Sarcomas

Bethany Cheree Prudner[1*], Fangdi Sun[1,2*], Jeffrey Charles Kremer[1], Jinbin Xu[3], Chaofeng Huang[3], Kiran Kumar Solingapuram Sai[3], Zachary Morgan[3], Hayden Leeds[3], Jonathan McConathy[3,4,5]✉, Brian Andrew Van Tine[1,4]✉

1. Division of Medical Oncology, Department of Internal Medicine, Washington University School of Medicine, St. Louis, MO, 63110, USA
2. Harvard Medical School, Cambridge, MA, 02115, USA
3. Department of Radiology, Washington University School of Medicine, St. Louis, MO, 63110, USA
4. Siteman Cancer Center, Washington University School of Medicine, St. Louis, MO, 63110, USA
5. Department of Radiology, University of Alabama at Birmingham, AL, 35249, USA

*There authors contributed equally to this work

✉ Corresponding authors: Brian A. Van Tine, M.D., Ph.D., 660 S Euclid, Campus Box 8007, St. Louis, MO 63110, Office: 314.747.8475; Fax: 314.747.9320; Email: bvantine@wustl.edu and Jonathan McConathy, MD., Ph.D., 619 19th St. South, JT 773, Birmingham, AL 35249, E-mail: jmcconathy@uabmc.edu

Received: 2017.07.25; Accepted: 2018.02.13; Published: 2018.03.07

Abstract

Rational: In a subset of cancers, arginine auxotrophy occurs due to the loss of expression of argininosuccinate synthetase 1 (ASS1). This loss of ASS1 expression makes cancers sensitive to arginine starvation that is induced by PEGylated arginine deiminase (ADI-PEG20). Although ADI-PEG20 treatment is effective, it does have important limitations. Arginine starvation is only beneficial in patients with cancers that are ASS1-deficient. Also, these tumors may metabolically reprogram to express ASS1, transforming them from an auxotrophic phenotype to a prototrophic phenotype and thus rendering ADI-PEG20 ineffective. Due to these limitations of ADI-PEG20 treatment and the potential for developing resistance, non-invasive tools to monitor sensitivity to arginine starvation are needed.

Methods: Within this study, we assess the utility of a novel positron emission tomography (PET) tracer to determine sarcomas reliant on extracellular arginine for survival by measuring changes in amino acid transport in arginine auxotrophic sarcoma cells treated with ADI-PEG20. The uptake of the ^{18}F-labeled histidine analogue, (*S*)-2-amino-3-[1-(2-[^{18}F]fluoroethyl)-1*H*-[1,2,3]triazol-4-yl]propanoic acid (AFETP), was assessed *in vitro* and *in vivo* using human-derived sarcoma cell lines. In addition, we examined the expression and localization of cationic amino acid transporters in response to arginine starvation with ADI-PEG20.

Results: *In vitro* studies revealed that in response to ADI-PEG20 treatment, arginine auxotrophs increase the uptake of L-[^{3}H]arginine and [^{18}F]AFETP due to an increase in the expression and localization to the plasma membrane of the cationic amino acid transporter CAT-1. Furthermore, *in vivo* PET imaging studies in mice with arginine-dependent osteosarcoma xenografts showed increased [^{18}F]AFETP uptake in tumors 4 days after ADI-PEG20 treatment compared to baseline.

Conclusion: CAT-1 transporters localizes to the plasma membrane as a result of arginine starvation with ADI-PEG20 in ASS1-deficient tumor cells and provides a mechanism for using cationic amino acid transport substrates such as [^{18}F]AFETP for identifying tumors susceptible to ADI-PEG20 treatment though non-invasive PET imaging techniques. These findings indicate that [^{18}F]AFETP-PET may be suitable for the early detection of tumor response to arginine depletion due to ADI-PEG20 treatment.

Key words: Arginine, Arginine Deiminase, ADI-PEG20, AFETP, CAT1

Introduction

Sarcomas are a rare and diverse group of malignancies with over 60 subtypes that arise from mesenchymal origin that can result in tumors of bone, muscle, cartilage or connective tissue (1, 2). In spite of advances in identifying and understanding the functional importance of genetic abnormalities within these tumors, cytotoxic chemotherapy still remains the standard of care for most locally advanced and metastatic sarcomas (3, 4). The risk of relapse remains high at 50%, with most of these representing metastatic failures with an overall survival of 12-14 months (1, 3). Despite the wide range of different subtypes within sarcoma, the silencing of arginine-succinate synthase 1 (ASS1) is found in approximately 90% of all sarcoma cases and is the most commonly altered gene in sarcoma (5). This silencing leads to ASS1 as a potential biomarker in several cancers (6, 7). As a result of the poor prognosis and very few available agents in sarcoma, there is a need for the development of new treatment strategies, including therapies based on sarcoma metabolism (1, 3, 5).

Dysregulation of tumor metabolism is emerging as a key event in cancer growth and tumorigenesis (8). The lack of ASS1 renders the tumors arginine auxotrophs, requiring exogenous arginine for cellular processes including growth, proliferation, and survival. Arginine is a semi-essential amino acid: although de novo synthesis can occur, it is not enough to maintain plasma levels of this amino acid, and so the main source for arginine is through dietary intake when ASS1 is deficient (9). Arginine is required for protein synthesis as well as an array of biosynthetic pathways including the synthesis of nitric oxide (NO), polyamines, and agmatine as well as the transamination of the amino acids proline and glutamate (10). ASS1 loss has been associated with decreased overall survival in ovarian cancer and myxoid fibrosarcoma, as well as reduced metastatic-free survival in osteosarcoma, implicating a tumor suppressor function for this metabolic gene (11-13). Exploiting the switch to arginine auxotrophy has led to clinical anticancer treatments where PEGylated arginine deiminase (ADI-PEG20) is used as an arginine-depleting therapy that induces nutrient starvation by enzymatically converting arginine to citrulline (7, 14-17). Recently it has been shown that this induced arginine starvation by ADI-PEG20 alters tumor metabolism by decreasing the tumor's dependence on the Warburg effect and increasing its dependence on oxidative phosphorylation (18).

When *de novo* arginine biosynthesis cannot occur due to the lack of ASS1 expression, cells need to transport arginine across the plasma membrane to maintain cellular functions, such as protein synthesis and proliferation (19, 20). Several families of specialized biological transporter systems can mediate the uptake of L-arginine and other cationic amino acids from the extracellular space including systems y^+, $b^{0,+}AT$, $ATB^{0,+}$ and y^+L. These transporters differ in mechanism of transport and specificity for cationic amino acids. The y^+ transport system is widely expressed and considered to be the major arginine transporter in most tissues and cells (21, 22). System y^+ activity is mediated by three different cationic amino-acid transporter proteins: (CAT)-1, CAT-2A/2B, and CAT-3, which are characterized by high affinity for cationic amino acids, sodium independence, and facilitated transport dependent on the intracellular substrate composition (23-25). Hatzoglou et al. showed that CAT-1 stability and translation increases when there is a limitation of amino acids (26). Finally, CAT-1 was implicated as the transporter in AML responsible for arginine uptake (27, 28), a finding that has not been investigated outside of AML.

Therefore, we hypothesized that arginine starvation will induce an increase in the expression and localization to the plasma membrane of an arginine transporter system, resulting in the augmentation of extracellular arginine uptake. Furthermore, we sought to exploit this biological response using the radiolabeled amino acid (*S*)-2-amino-3-[1-(2-[^{18}F]fluoroethyl)-1*H*-[1,2,3]triazol-4-yl]propanoic acid (AFETP) as a positron emission tomography (PET) imaging agent to detect the upregulation of amino acid transport by tumor cells deprived of extracellular arginine. [^{18}F]AFETP is structurally similar to the natural amino acid L-histidine and enters cells in part through the cationic amino acid transporters (29, 30). Previous studies have shown promising imaging properties in rodent models of high grade glioma. These properties make [^{18}F]AFETP well-suited to non-invasively monitor changes in cationic amino acid transport through small animal PET in mice with the potential for clinical translation for imaging this phenomenon in cancer patients (29). As ASS1-deficient tumors exposed to ADI-PEG20 monotherapy develop resistance through the re-expression of ASS1, [^{18}F]AFETP-PET could be a useful clinical tool in patients being treated with ADI-PEG20 for early response evaluation and to detect the development of resistance to ADI-PEG20 therapy (5, 31).

Results

Sarcoma cell lines frequently lack expression of ASS1

As the lack of ASS1 expression is generally

associated with sensitivity to ADI-PEG treatment, expression levels were assessed in human sarcoma tumors (5). Bean et al. revealed that approximately 90% of sarcoma tumors have decreased or loss of ASS1 expression. To further expand on the immunohistochemical analysis that showed a frequent loss of ASS1 expression in sarcoma human tumors, a panel of sarcoma cell lines were assessed for the expression status of ASS1. Western blot analysis revealed that ASS1 is not significantly expressed in the SKLMS1 cell line and is expressed to a lesser extent in MNNG as compared to MG63, a cell line resistant to treatment with ADI-PEG20 (5). Furthermore, ASS1 expression was either increased or expressed upon ADI-PEG20 treatment (**Fig 1A**). The effect of ADI-PEG20 on cell growth, *in vitro*, was assessed in both ASS-positive sarcoma cell lines and those lacking expression of the enzyme. A clear correlation of ASS1 expression with or without ADI-PEG treatment on cell growth was observed. For the ASS1-negative sarcoma cell lines, SKLMS1 and MNNG, cell growth was arrested in comparison with the ASS1-positive MG63 cell line when they were treated with ADI-PEG20 (**Fig 1B**; mean ± SD (%) for untreated cells: 100 ± 4.8 (SKLMS1),100 ± 1.5 (MNNG), 100 ± 5.1 (MG63) vs. ADI-PEG20-treated cells: 40 ± 4.5 (SKLMS1), 51 ± 1.8 (MNNG), 98 ± 4.9 (MG63). In ASS1-negative cell lines unable to make arginine, normalized L-[^{3}H]arginine uptake increased by 2.1 ± 0.8 fold (SKLMS1) and 3.2 ± 0.5 fold (MMNG) compared to control conditions after 72 hours of ADI-PEG20 treatment while the ASS1-positive cell line MG63 showed a 0.7 ± 0.2 fold change in normalized L-[^{3}H]arginine uptake with ADI-PEG20 treatment (see **Fig 1C**). Taken together, these results identify a subpopulation of sarcoma cell lines that are arginine auxotrophs due to the decreased enzymatic activity of ASS1.

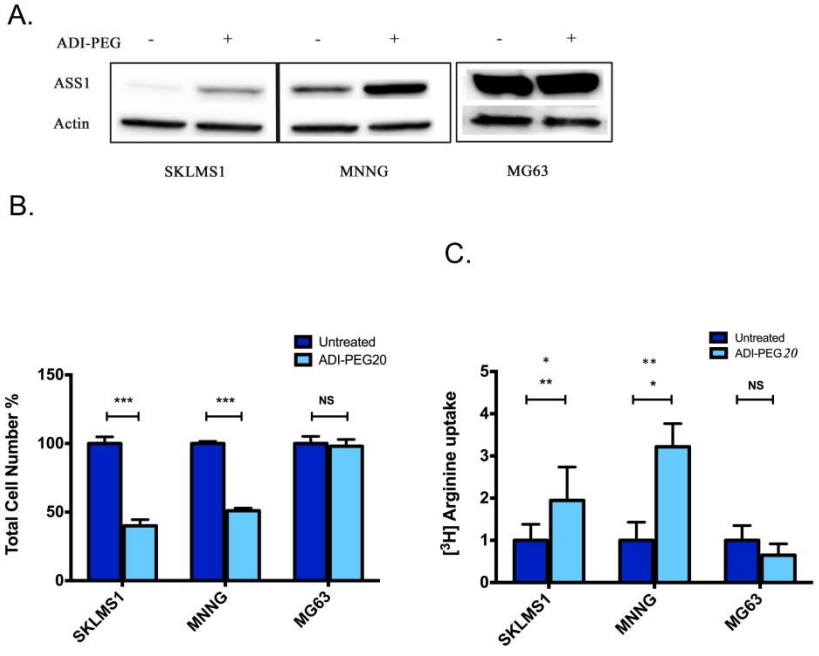

Figure 1. ASS1 levels correlate with ADI-PEG20 response in sarcoma cell lines. (**A**) Western blot analysis of ASS1 expression in SKLMS1, MNNG and MG63 cell lines in the presence of ADI-PEG20 treatment (72 h). Actin was used as a loading control. (**B**) Total cell count of SKLMS1, MNNG and MG63 after 72 h of ADI-PEG20 treatment. The total percentage of cells was normalized to the untreated control. (**C**) L-[^{3}H]Arginine uptake normalized to control conditions after 72 h of arginine starvation in SKLMS1, MNNG and MG63. All experiments were done in biological triplicate. ***p<0.001, **p<0.01, *p<0.05

Protein expression of cationic amino acid transporters in sarcoma cell lines

Due to the increased uptake of arginine in the ASS1-deficient cell lines upon arginine deprivation, the question of whether the expression levels of cationic amino acid transporters changed relative to ADI-PEG20 treatment in sarcoma cell lines was addressed. Immunoblot analysis of seven transporters, CAT-1, CAT-2, CAT-3, y$^+$LAT1, y$^+$LAT2, b^{o+}AT and ATB^{0+0}, demonstrated that only CAT-1 transporter expression was increased in response to ADI-PEG20 treatment, whereas CAT-2, CAT-3, y+LAT1, y$^+$LAT2, b^{o+}AT and ATB$^{0,+}$ expression levels were found to remain constant or decrease upon arginine starvation (**Fig 2**). CAT-1 protein expression was also found to increase in MG63 in response to extracellular arginine depletion with ADI-PEG20, but this finding did not correlate with increased extracellular L-[^{3}H]arginine uptake (**Fig 1C**).

Membrane localization of the cationic amino acid transporters in sarcoma cell lines by IF

As only CAT-1 protein expression changed expression pattern in response to arginine starvation, we examined the subcellular localization of the y$^+$ transporters in response to ADI-PEG20 treatment using semi-quantitative immunofluorescence labeling (32). In response to ADI-PEG20 treatment, CAT-1 was observed to alter its localization, with increased abundance seen at the plasma membrane (**Fig 3**). Though CAT-3 expression could not be reliably determined by IF after multiple attempts, the other five cationic amino acid transporters examined were not dramatically altered by ADI-PEG20 treatment (**Fig 3**). This demonstrates that CAT-1 is the critical arginine transporter implicated in the response to ADI-PEG20 treatment in ASS1-deficient sarcomas.

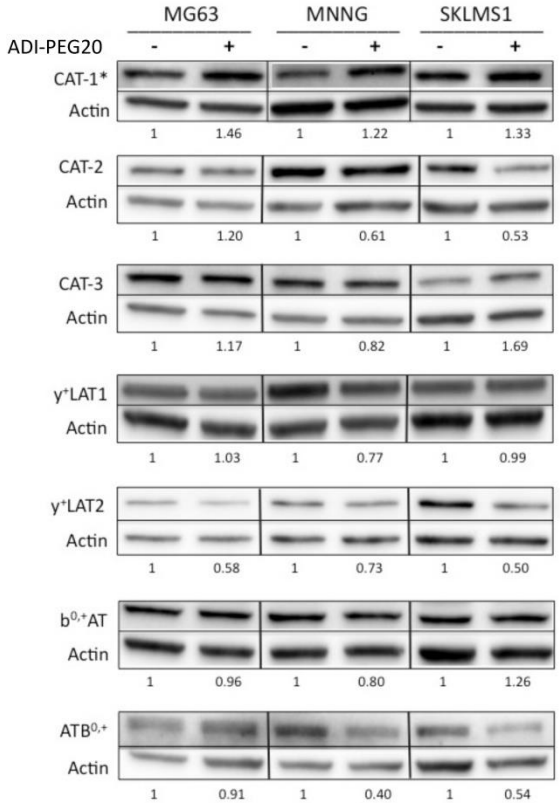

Figure 2. Cationic amino acid transporters' expression in response to ASI-PEG20. Western blot analysis of the expression of CAT-1, CAT-2, CAT-3, y^+LAT1, y^+LAT2, $b^{0,+}$AT and $ATB^{0,+}$ in MG63, MNNG and SKLMS1 after 72 h of ADI-PEG20 treatment. All experiments were done in biological triplicate.

Uptake of [^{18}F]AFETP increases after ADI-PEG20 treatment *in vitro*

To determine if the translocation of CAT-1 to the plasma membrane following ADI-PEG20 treatment could be exploited for *in vivo* imaging, we measured the cellular uptake of the ^{18}F-labeled amino acid AFETP *in vitro*. [^{18}F]AFETP is structurally similar to L-histidine (**Fig 4A**). After 72 h of ADI-PEG20-induced arginine starvation, [^{18}F]AFETP uptake was increased in the ADI-sensitive SKLMS1 and MNNG cell lines by 2.2 ± 0.4 and 1.5 ± 0.3 respectively, but not the ADI-resistant cell line MG63 where a 1.1 ± 0.1 fold change was observed with ADI-PEG20 treatment. These results are similar to those obtained with L-[^{3}H]arginine and demonstrate that [^{18}F]AFETP can be used as a surrogate for ADI-PEG20 response in cell lines that are sensitive to ADI-PEG20 (see **Fig 4B**). Finally, as there was not an increase in [^{18}F]AFETP uptake in the MG63 ADI-PEG20-resistant cell line, [^{18}F]AFETP may be a useful tool for determining when resistance to ADI-PEG20 evolves *in vivo*. These results trended in the same direction as those observed with L-[^{3}H]arginine (**Fig 1B, C**).

[^{18}F]AFETP-PET shows increased uptake after arginine depletion *in vivo*

To test the ability of [^{18}F]AFETP to monitor response to ADI-PEG20 *in vivo*, small animal PET studies were performed before and after ADI-PEG20 treatment in a mouse model of arginine-dependent sarcoma. ASS1-negative SKLMS1 cells were xenografted into nude mice (5). Once tumors volume reached between 200-500 mm^3, mice were treated with 320 IU/m^2 (29.1 mg/m^2) ADI-PEG20 once every three days. [^{18}F]AFETP-PET imaging in mice with SKLMS1 tumor xenografts was performed immediately prior to starting ADI-PEG20 treatment and again at day 2 (after 1 ADI-PEG20 treatment) and day 4 (after 2 ADI-PEG20 treatments) to determine if [^{18}F]AFETP uptake increased after systemic arginine depletion. In all animals, the tumors were clearly visualized above background tissues at baseline and after treatment with ADI-PEG20. These studies also demonstrated visually increased tracer uptake in the most of tumor xenografts at day 4 of ADI-PEG20 treatment (**Fig 5A, B**). The average tumor to skeletal muscle ratios ± SD were 2.3 ± 0.6 on day 0 (prior to ADI-PEG20), 2 and 4, 3.0 ± 1.5 on day 2 of ADI-PEG20 administration, and 3.2 ± 1 on day 4 of ADI-PEG20 administration (**Fig 5B**; n=6 animals). The average tumor standardized uptake values (SUVs) ± SD were 0.63± 0.06 on day 0, 0.72 ± 0.3 on day 2, and 0.74 ± 0.2 on day 4.

Changes in tumor size can affect PET measurements of standardized uptake values (SUVs) due to partial volume averaging, particularly when lesions are close to the resolution limits of PET. To address this potential confounding variable, the maximum axial dimensions of each tumor were measured (2 perpendicular measurements for each tumor) prior to beginning ADI-PEG20 administration (day 0) and again after 4 days of ADI-PEG20 treatment (day 4). The tumors ranged in axial dimensions from 6x4 mm to 17x12 mm on day 0 and from 7x4 mm to 18x13 mm on day 4. The sums of the axial bidimensional measurements at day 0 and day 4 were compared, and the sum of measurements increased by an average of 6.4 ± 4% and 1.3 ± 1 mm by day 4. Given this small increase in size and the ~1.5-2 mm resolution of the small animal PET scanners used in this study, the observed increase in tumor size is unlikely to account for the difference in tumor to muscle ratios, which increased by an average of 36% by day 4. The apparent increase in tumor size in **Fig. 5A** is primarily due to increased [^{18}F]AFETP uptake rather than increased tumor size. However, the present studies do not entirely exclude a contribution of increasing tumor size to the increased tumor to muscle ratios observed at day 4 of ADI-PEG20 therapy.

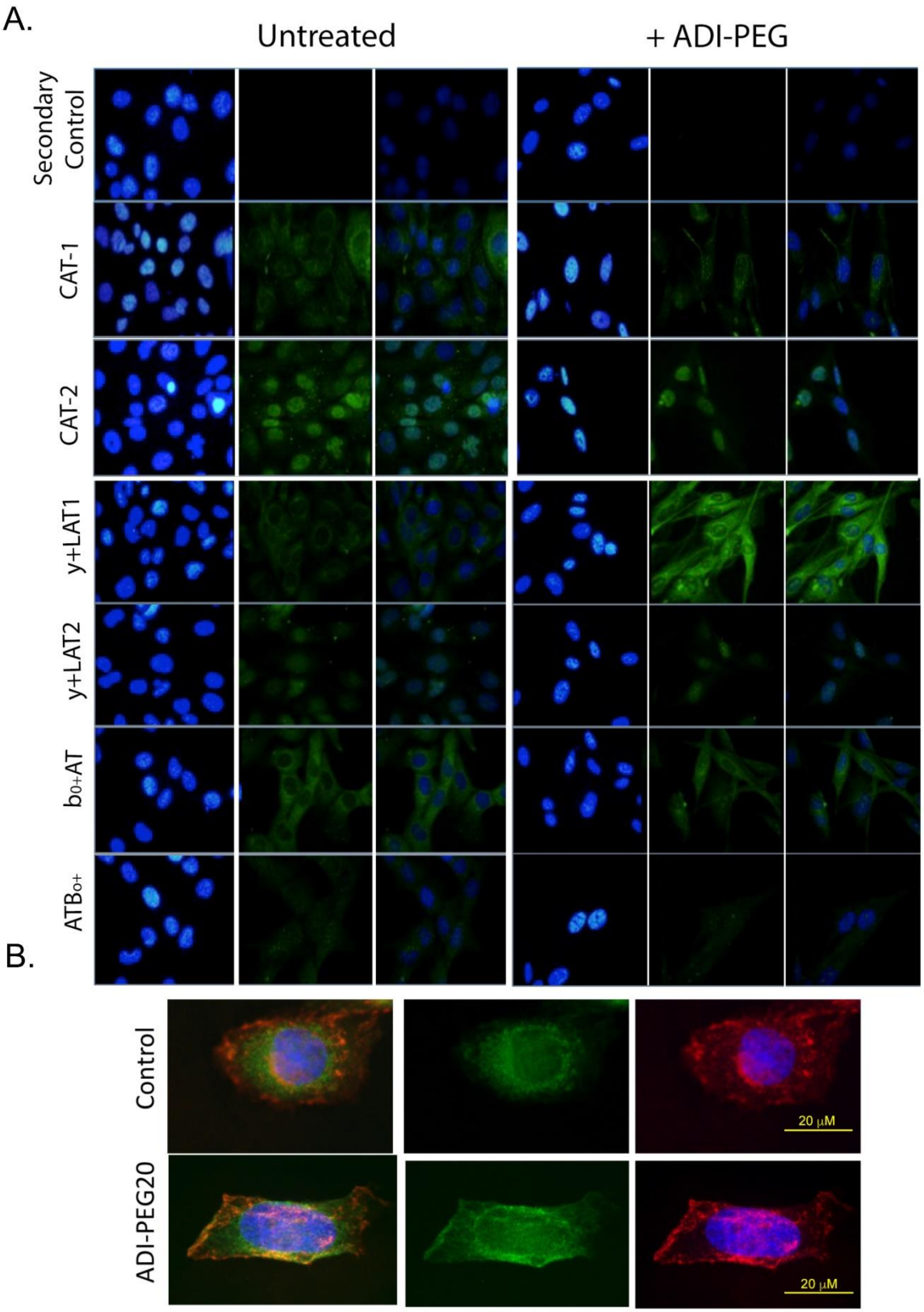

Figure 3. CAT1 translocates to the plasma membrane in response to ADI-PEG20 treatment. (**A**) Immunofluorescence of CAT1, CAT-2, CAT-3, y^+LAT1, y^+LAT2, $b^{0,+}$AT and $ATB^{0,+}$ expression in SKLMS1 after 72 h of ADI-PEG20 treatment. Green is FITC secondary label, blue is DAPI. Control for the secondary antibody demonstrates no signal above autofluorescence. All images are at 60x. Scale bar, 20 μm. (**B**) Immunofluorescence of CAT1 expression in SKLMS1 after 72 h of ADI-PEG20 treatment. Green is FITC secondary label, blue is DAPI, red is TRITC for wheat germ agglutinin (WGA) for plasma membrane staining. Images are merged to show overlap between CAT-1 translocation and plasma membrane staining. Scale bar, 20 μm.

Discussion

Sarcomas comprise over 60 different types of tumors, whose underlying biological diversity makes the development of a common and effective therapeutic across a wide range of subtypes very challenging. Historically, common mutations have included TP53, which occurs in only up to 50% of sarcomas, and PTEN loss, effecting only 30% of certain subtypes (32, 33). Only recently has it been demonstrated that approximately 90% of all sarcomas are ASS1-deficient; this discovery has led to the development of targeted therapies based on a common metabolic defect (5). As treatment of ASS1-deficient sarcomas with ADI-PEG20 monotherapy allows only for the inhibition of cell growth, combination therapies based on the metabolic changes induced by ADI-PEG20 will need to be carefully developed (11, 12).

Outside of the sarcoma field, ADI-PEG20 has been used in combination with other anti-proliferative drugs such as cisplatin, gemcitabine, and pemetrexed (34, 35). The success of these combinations has branched out into treating other cancers and is currently being assessed in clinical trials of advanced hepatocellular carcinoma, refractory small cell lung cancer, malignant pleural mesothelioma, prostate cancer, non-Hodgkin's lymphoma, and acute myeloid leukemia (36, 37). As ASS1 is expressed in most normal tissues, therapeutically exploiting this enzymatic deficiency is highly desirable, as the toxicity to normal tissues should be less than other non-specific chemotherapies. The availability of an imaging biomarker suitable for preclinical and human use to assess the consequences and biological efficacy of arginine starvation is greatly needed to optimize the use of ADI-PEG20 for cancer therapy.

In our study, the ^{18}F-labeled amino acid AFETP was used as a surrogate to monitor the upregulation of amino acids transport in response to ADI-PEG20 in an established preclinical animal model of sarcoma. Our overall findings are modeled in **Fig 6**. The *in vitro* studies examined the auxotrophic nature of ASS1-deficient cell lines, which are known to be more sensitive to ADI-PEG20 treatment. SKLMS1 and MNNG had a significant increase in L-[H^3]arginine uptake after ADI-PEG20 treatment, as opposed to the insignificant change seen in the ASS1 expressing cell line MG63. To assess the mechanism underlying the increased arginine uptake, amino acid transporter expression was evaluated, with a slight increase in the expression of CAT-1 observed. In addition, IF was done to see if transporter translocation changes occurred upon ADI-PEG20 treatment, as localization may be more important than total expression for arginine uptake. Again, the results demonstrated that only CAT-1 translocated to the plasma membrane in response ADI-PEG20 treatment. Although CAT-1 expression did increase in the ASS1 expressing cell line MG63, this increase in expression did not correlate with an increased uptake of L-[H^3]arginine. This would suggest that CAT1 expression and translocation may be controlled by sensing extracellular arginine concentrations, given the fact that MG63 can produce its own intracellular arginine because of its high ASS1 expression. Further studies are needed to validate this hypothesis.

ADI-PEG20 induces a starvation response that leads to the destruction of various proteins in an effort to provide a source of arginine (5). As a result, we find that some of the cationic transports may be a target of this process. Despite the fact that there was a small decrease in the

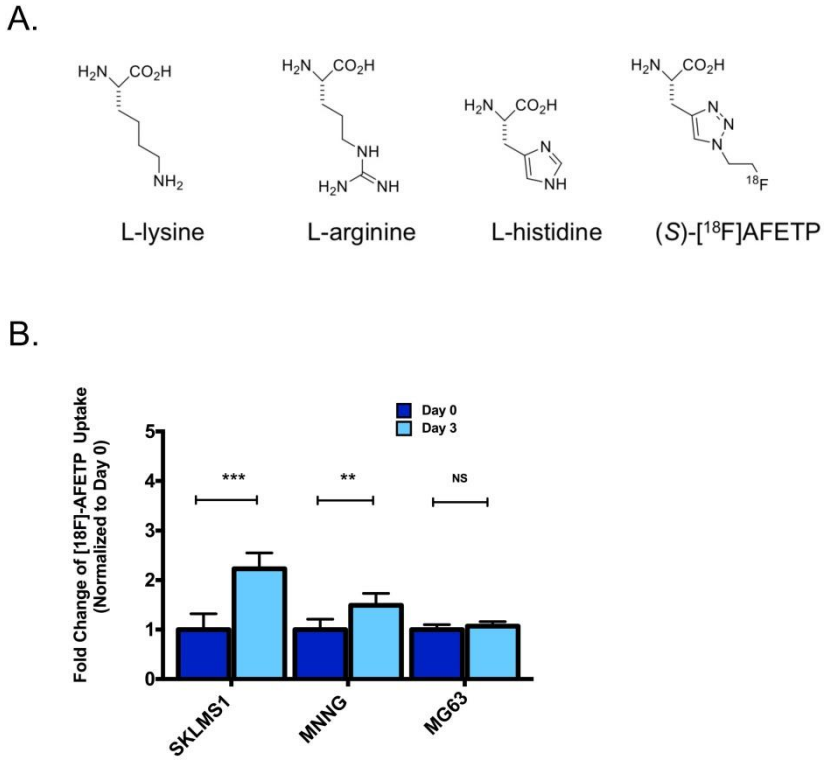

Figure 4. AFETP uptake increases in response to ADI-PEG20 in ASS1-deficient cells *in vitro*. (**A**) AFETP is structurally similar to histidine and is recognized by cationic and neutral amino acid transporters. The structure of the other cationic amino acids L-lysine and L-arginine are shown. (**B**) [^{18}F]AFETP uptake normalized to control conditions in SKLMS1, MNNG and MG63 cell lines after 72 h of ADI-PEG20 treatment. All experiments were done in biological triplicate. ***p<0.001, **p<0.01, *p<0.05.

expression of y+LAT2 and ATB0,+, this result does not appear to alter the ability of SKLMS1 or MNNG to accumulate [18F]AFETP or L-[3H]arginine intracellularly. Altogether, this result could suggest that selective CAT-1 substrates inhibitors may be effective in improving the response to ADI-PEG20 for induced arginine starvation.

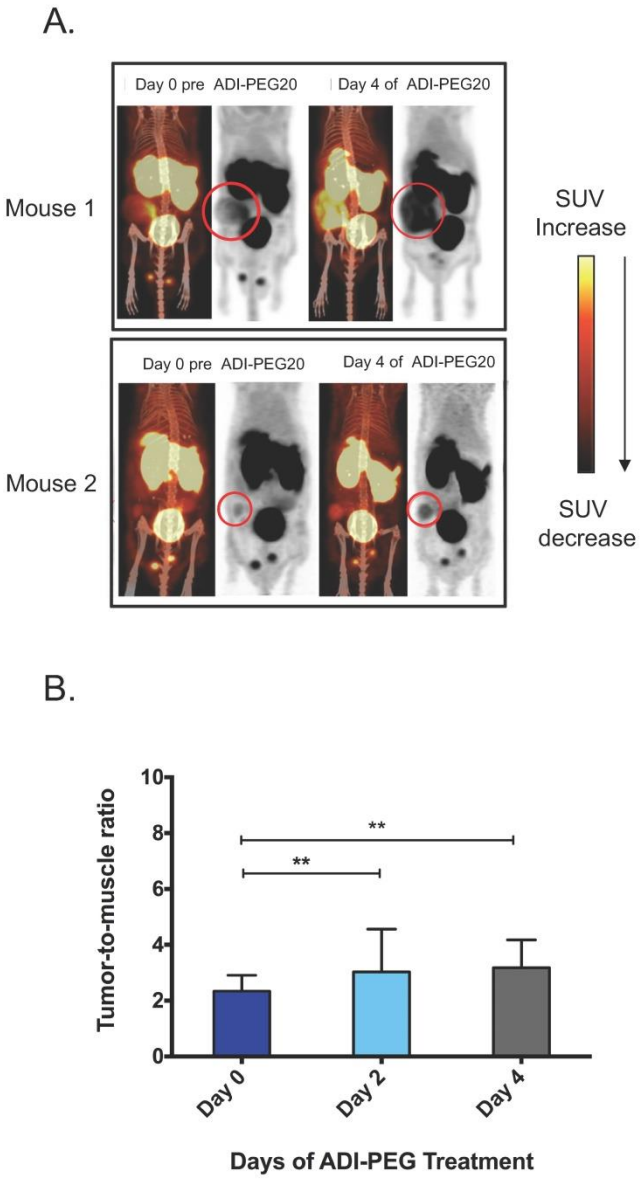

Figure 5. Tumor uptake of AFETP increases in response to ADI-PEG20 treatment *in vivo*. (**A**) Two representative model mice at day 0 (baseline) and day 4 of ADI-PEG20 treatment. In addition, signal was seen in the liver, bladder and testes. (**B**) Tumor to skeletal muscle ratios observed with [18F]AFETP *in vivo*. N=6 mice. ***p<0.001, **p<0.01, *p<0.05.

PET use after treatment with ADI-PEG20 in ASS1-deficient cancers has only been evaluated in a few cases (38-41). The glucose analogue [18F]FDG does not appear to be useful for monitoring response to ADI-PEG20 treatment, as demonstrated by the decreased uptake in bladder cancer, which could be due to the rewiring of glucose metabolism by the treatment ADI-PEG20 and not due to tumor death (18, 22). The uptake of [18F]AFETP is more closely related to the mechanism of cellular arginine uptake in response to ADI-PEG20 than is glucose metabolism measured with [18F]FDG. This study demonstrated that uptake of [18F]AFETP increased as opposed to decreased in response to arginine starvation. Given the possible heterogeneity of ASS1 expression in patients with multiple tumors and the unknown time frame of resistance due to ASS1 expression in patients with ASS1-deficient tumors, changes in [18F]AFETP uptake may be an early indication of tumor response to treatment. A potential limitation of [18F]AFETP for this application is the transport of this amino acid by both cationic and neutral amino acid transporters. Finally, formal clinical trials of [18F]AFETP and ADI-PEG20 will be needed to assess efficacy in patients with ASS1-deficient tumors.

Materials and Methods

Cell Culture

Cell lines SKLMS1, MNNG and MG63 were purchased from ATCC (Manassas, VA). Cell lines were cultured at 37 °C and 5% CO_2 in Modified Eagle Medium (MEM) (Life Technologies, Grand Island, NY) supplemented with 10% FBS and Penicillin-Streptomycin 100x (10,000 U/mL) (Life Technologies, Grand Island, NY).

Western Blotting

Whole-cell lysates were prepared using RIPA cell lysis buffer (Cell Signaling, Danvers, MA). Protein concentration was calculated using Bradford assay and 40 µg of protein was loaded and run on SDS-PAGE and transferred to polyvinylidene difluoride (PVDF) membranes (Bio-Rad, Hercules, CA). Membranes were blocked with 5% bovine serum albumin or low-fat milk and incubated with the following antibodies: CAT-1, CAT-2, CAT-3, y+LAT-1, y+LAT-2, b0,+AT, ATB0,+ (Santa Cruz Biotechnology, Dallas, TX).

Immunofluorescence

5000 cells were seeded in 2-well chamber slides. Cells were treated with 1 µg/mL ADI-PEG20 (Polaris Inc, San Diego, CA, USA) for 72 h. Cells were washed twice with 1x PBS and fixed with 4% PFA in 1x PBS for 10 min. Cells were washed three times with 1x PBS and blocked with 50% goat serum in 1x PBS for 30 min at 37 °C. Primary antibodies were then added for 1 h at 37 °C, washing three times for 5 min. Secondary antibodies were added for 1 h at 37 °C. After a final three washes for 5 min, cells were mounted in Prolong Gold with DAPI (Vector, Olean, NY). Cells were

imaged with an Olympus microscope and an Olympus DP72 camera. Camera settings were 128 ms for all FITC images. All images were assembled with Photoshop (Elements 13) and all changes to the FITC images were uniformly applied for figure clarity Photographs were equally adjusted in the green channel for printing clarity by changes "levels" so that the maximal intensity of the control figure was the given the maximal grey value. This was applied equally to the entire dataset. The nuclear stain in blue was adjusted non-uniformly as it is a nuclear marker to be used as a cellular special reference and not part of the experiment.

Uptake Assays

Cell lines were seeded at $1x10^5$ cells per well in 24-well plates (Corning Costar). The following assay buffers were used for the cell uptake studies: For L-[^{3}H]arginine uptake assays, 7.4 MBq (200 µCi) of L-[^{3}H]arginine (L-[2,3,4-^{3}H]arginine monohydrochloride (1.48–2.59 TBq)/mmol, 37 MBq/mL, Perkin Elmer, Waltham, MA) in 2% ethanol/water stock solution was diluted in 15.5 mL of assay buffer (105 mM sodium chloride, 3.8 mM potassium chloride, 1.2 mM potassium bicarbonate, 25 mM sodium phosphate dibasic, 0.5 mM calcium chloride dihydrate, 1.2 mM magnesium sulfate, and 5.6 mM D-glucose adjusted to pH 7.4) at a concentration of 0.5 MBq/mL (13 µCi/mL). For [^{18}F]AFETP uptake assays, ^{18}F-labeled amino acid AFETP was prepared as previously reported (29, 30), and a stock solution of 74 MBq/mL (2 mCi/mL) of [^{18}F]AFETP in water was diluted to a concentration of ~1.5 MBq/mL (40 µCi/mL).

The cell uptake assays were initiated by discarding the culture media and then rinsing the cells twice with 2 mL of assay buffer at 37°C without radiotracer. Aliquots of assay buffer containing L-[^{3}H]arginine (0.2 mL) or [^{18}F]AFETP (0.4 mL) were then added to each well and allowed to incubate at 37 °C for 5 min. The assay buffer containing the radiotracer was removed, and the wells were rinsed twice with 1 mL of ice-cold assay buffer without radiotracer. The cells were lysed by treating each well with 0.3 mL aliquots of aqueous 0.2% sodium dodecyl sulfate (SDS) in 0.2 M sodium hydroxide (NaOH) and then shaking the 24-well plates gently at room temperature for 45 min. Protein concentrations in each well were measured in triplicate (30 µL aliquots) using the Pierce bicinchoninic acid (BCA) protein assay kit method (Rockford, IL).

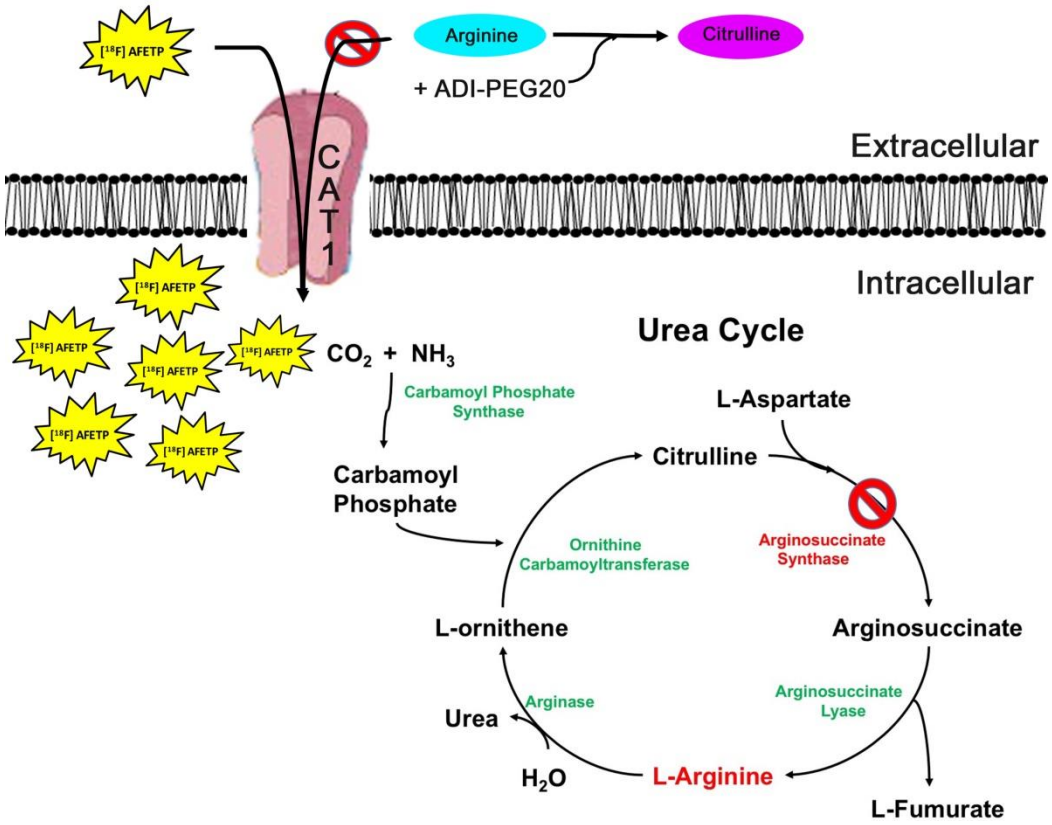

Figure 6. Model of [^{18}F]AFETP uptake in response to ADI-PEG20 treatment. In the presence of ADI-PEG20, extracellular arginine is converted to citrulline. In ASS1-deficient tumors, depletion of the extracellular pool of arginine causes an increase in the translocation of CAT1 to the plasma membrane. This allows for the PET tracer [^{18}F]AFETP to be taken up into the cell, making this a useful tool for assessing biological response to ADI-PEG20 treatment.

For the [^{18}F]AFETP assays, the radioactivity in 150 µL of lysate from each well and in radioactive standards was measured as counts per minute (cpm) using a gamma counter (2480 Wizard^2, Perkin Elmer). The cpm measurements were decay-corrected for elapsed time. For L-[^{3}H]arginine assays, a 150 µL aliquot of lysate from each well was added to 2.5 mL of Biosafe II liquid scintillation fluid (Research Products International Corp, Mt. Prospect, IL) in 3 mL vials. The vials were then shaken vigorously and allowed to stand overnight. The radioactivity in the vials was then measured as cpm using a liquid scintillation counter (LS6500, Beckman Coulter Inc, Fullerton CA). For both [^{18}F]AFETP and L-[^{3}H] arginine assays, the cpm measurements were normalized to the protein concentration in each well. Assays were performed in triplicate and the values for the ADI-PEG20-treated cells were expressed as the percent uptake relative to the untreated condition for each cell line. The data is depicted as average of percent uptake used for statistical analysis.

Small animal PET imaging

All xenograft and small animal imaging experiments were approved by the Animal Studies Committee at Washington University School of Medicine. Male nude mice with subcutaneously implanted SKLMS1 tumor xenografts (n=6) underwent small animal PET imaging immediately prior to ADI-PEG20 administration (day 0) and days 2 and 4 after beginning ADI-PEG20. For each PET study, the mice were anesthetized with 1% isoflurane/oxygen followed by dynamic PET acquisition at 0-60 min after intravenous tail injection of 10-12 MBq of [^{18}F]AFETP using INVEON and MicroPET Focus 220 systems. The animals were allowed to feed ad libitum prior to the [^{18}F]AFETP studies. The animals were maintained at 37 ^{o}C during the study using a warming lamp. Computed tomography (CT) images were also acquired with the INVEON system.

The small animal PET data were analyzed by manually drawing 3-dimensional regions of interest (ROIs) over the tumor identified on the PET studies with correlation to CT to confirm the tumor location. ROIs for normal skeletal muscle were drawn over the lower extremity based on the CT images. The uptake data were expressed as mean standardized uptake values (SUVs) for each ROI. Tumor to skeletal muscle ratios were calculated by dividing the mean SUV in of the tumor by the mean SUV of the skeletal muscle ROI for each animal. The average of the SUVs in tumor and muscle and the average of the tumor-to-muscle ratios at 50-60 min after injection of [^{18}F]AFETP were compared using 2-tailed t-tests.

Abbreviations

ASS1: Argininosuccinate synthetase 1; ADI-PEG20: PEGylated arginine deiminase; PET: positron emission tomography; ^{18}F: ^{18}F-labeled histidine analogue, AFETP: (*S*)-2-amino-3-[1-(2-[^{18}F]fluoroethyl)-1*H*-[1,2,3]triazol-4-yl]propanoic acid; CAT-1: cationic amino acid transporter; NO: nitric oxide.

Acknowledgements

The Siteman Cancer Center is supported in part by NCI Cancer Center Support Grant #P30 CA91842. This research was funded by the National Cancer Institute (K08CA154790; P50CA94056).

Competing Interests

The authors have declared that no competing interest exists.

References

1. Clark MA, Fisher C, Judson I, Thomas JM. Soft-tissue sarcomas in adults. N Engl J Med. 2005;353(7):701-11.
2. Demetri GD, Antonia S, Benjamin RS, Bui MM, Casper ES, Conrad EU, 3rd, et al. Soft tissue sarcoma. J Natl Compr Canc Netw. 2010;8(6):630-74.
3. Demetri GD, Elias AD. Results of single-agent and combination chemotherapy for advanced soft tissue sarcomas. Implications for decision making in the clinic. Hematol Oncol Clin North Am. 1995;9(4):765-85.
4. Jain S, Xu R, Prieto VG, Lee P. Molecular classification of soft tissue sarcomas and its clinical applications. Int J Clin Exp Pathol. 2010;3(4):416-28.
5. Bean GR, Kremer JC, Prudner BC, Schenone AD, Yao JC, Schultze MB, et al. A metabolic synthetic lethal strategy with arginine deprivation and chloroquine leads to cell death in ASS1-deficient sarcomas. Cell death & disease. 2016;7(10):e2406.
6. Szlosarek PW, Grimshaw MJ, Wilbanks GD, Hagemann T, Wilson JL, Burke F, et al. Aberrant regulation of argininosuccinate synthetase by TNF-alpha in human epithelial ovarian cancer. Int J Cancer. 2007;121(1):6-11.
7. Dillon BJ, Prieto VG, Curley SA, Ensor CM, Holtsberg FW, Bomalaski JS, et al. Incidence and distribution of argininosuccinate synthetase deficiency in human cancers: a method for identifying cancers sensitive to arginine deprivation. Cancer. 2004;100(4):826-33.
8. Hanahan D, Weinberg RA. Hallmarks of cancer: the next generation. Cell. 2011;144(5):646-74.
9. Castillo L, Chapman TE, Sanchez M, Yu YM, Burke JF, Ajami AM, et al. Plasma arginine and citrulline kinetics in adults given adequate and arginine-free diets. Proc Natl Acad Sci U S A. 1993;90(16):7749-53.
10. Delage B, Fennell DA, Nicholson L, McNeish I, Lemoine NR, Crook T, et al. Arginine deprivation and argininosuccinate synthetase expression in the treatment of cancer. Int J Cancer. 2010;126(12):2762-72.
11. Kobayashi E, Masuda M, Nakayama R, Ichikawa H, Satow R, Shitashige M, et al. Reduced argininosuccinate synthetase is a predictive biomarker for the development of pulmonary metastasis in patients with osteosarcoma. Mol Cancer Ther. 2010;9(3):535-44.
12. Huang HY, Wu WR, Wang YH, Wang JW, Fang FM, Tsai JW, et al. ASS1 as a novel tumor suppressor gene in myxofibrosarcomas: aberrant loss via epigenetic DNA methylation confers aggressive phenotypes, negative prognostic impact, and therapeutic relevance. Clin Cancer Res. 2013;19(11):2861-72.
13. Nicholson LJ, Smith PR, Hiller L, Szlosarek PW, Kimberley C, Sehouli J, et al. Epigenetic silencing of argininosuccinate synthetase confers resistance to platinum-induced cell death but collateral sensitivity to arginine auxotrophy in ovarian cancer. Int J Cancer. 2009;125(6):1454-63.
14. Izzo F, Marra P, Beneduce G, Castello G, Vallone P, De Rosa V, et al. Pegylated arginine deiminase treatment of patients with unresectable hepatocellular carcinoma: results from phase I/II studies. Journal of clinical oncology : official journal of the American Society of Clinical Oncology. 2004;22(10):1815-22.
15. Ascierto PA, Scala S, Castello G, Daponte A, Simeone E, Ottaiano A, et al. Pegylated arginine deiminase treatment of patients with metastatic melanoma: results from phase I and II studies. Journal of clinical oncology : official journal of the American Society of Clinical Oncology. 2005;23(30):7660-8.
16. Glazer ES, Piccirillo M, Albino V, Di Giacomo R, Palaia R, Mastro AA, et al. Phase II study of pegylated arginine deiminase for nonresectable and metastatic hepatocellular carcinoma. J Clin Oncol. 2010;28(13):2220-6.

17. Feun LG, Marini A, Walker G, Elgart G, Moffat F, Rodgers SE, et al. Negative argininosuccinate synthetase expression in melanoma tumours may predict clinical benefit from arginine-depleting therapy with pegylated arginine deiminase. Br J Cancer. 2012;106(9):1481-5.
18. Kremer JC, Prudner BC, Lange SE, Bean GR, Schultze MB, Brashears CB, et al. Arginine Deprivation Inhibits the Warburg Effect and Upregulates Glutamine Anaplerosis and Serine Biosynthesis in ASS1-Deficient Cancers. Cell reports. 2017;18(4):991-1004.
19. Lee J, Ryu H, Ferrante RJ, Morris SM, Jr., Ratan RR. Translational control of inducible nitric oxide synthase expression by arginine can explain the arginine paradox. Proc Natl Acad Sci U S A. 2003;100(8):4843-8.
20. Esch F, Lin KI, Hills A, Zaman K, Baraban JM, Chatterjee S, et al. Purification of a multipotent antideath activity from bovine liver and its identification as arginase: nitric oxide-independent inhibition of neuronal apoptosis. J Neurosci. 1998;18(11):4083-95.
21. McCracken AN, Edinger AL. Nutrient transporters: the Achilles' heel of anabolism. Trends Endocrinol Metab. 2013;24(4):200-8.
22. Allen MD, Luong P, Hudson C, Leyton J, Delage B, Ghazaly E, et al. Prognostic and therapeutic impact of argininosuccinate synthetase 1 control in bladder cancer as monitored longitudinally by PET imaging. Cancer Res. 2014;74(3):896-907.
23. Kim JW, Closs EI, Albritton LM, Cunningham JM. Transport of cationic amino acids by the mouse ecotropic retrovirus receptor. Nature. 1991;352(6337):725-8.
24. White MF, Gazzola GC, Christensen HN. Cationic amino acid transport into cultured animal cells. I. Influx into cultured human fibroblasts. J Biol Chem. 1982;257(8):4443-9.
25. White MF, Christensen HN. The two-way flux of cationic amino acids across the plasma membrane of mammalian cells is largely explained by a single transport system. J Biol Chem. 1982;257(17):10069-80.
26. Hatzoglou M, Fernandez J, Yaman I, Closs E. Regulation of cationic amino acid transport: the story of the CAT-1 transporter. Annu Rev Nutr. 2004;24:377-99.
27. Shima Y, Maeda T, Aizawa S, Tsuboi I, Kobayashi D, Kato R, et al. L-arginine import via cationic amino acid transporter CAT1 is essential for both differentiation and proliferation of erythrocytes. Blood. 2006;107(4):1352-6.
28. Miraki-Moud F, Ghazaly E, Ariza-McNaughton L, Hodby KA, Clear A, Anjos-Afonso F, et al. Arginine deprivation using pegylated arginine deiminase has activity against primary acute myeloid leukemia cells *in vivo*. Blood. 2015;125(26):4060-8.
29. Sai KK, Huang C, Yuan L, Zhou D, Piwnica-Worms D, Garbow JR, et al. 18F-AFETP, 18F-FET, and 18F-FDG imaging of mouse DBT gliomas. J Nucl Med. 2013;54(7):1120-6.
30. McConathy J, Zhou D, Shockley SE, Jones LA, Griffin EA, Lee H, et al. Click Synthesis and Biologic Evaluation of (*R*)- and (*S*)-2-Amino-3-[1-(2-[^{18}F]fluoroethyl)-1*H*-[1,2,3]Triazol-4-yl]Propanoic Acid for Brain Tumor Imaging with Positron Emission Tomography. Mol Imaging. 2010;9(6):329-42.
31. Long Y, Tsai WB, Wangpaichitr M, Tsukamoto T, Savaraj N, Feun LG, et al. Arginine deiminase resistance in melanoma cells is associated with metabolic reprogramming, glucose dependence, and glutamine addiction. Mol Cancer Ther. 2013;12(11):2581-90.
32. Movva S, Wen W, Chen W, Millis SZ, Gatalica Z, Reddy S, et al. Multi-platform profiling of over 2000 sarcomas: identification of biomarkers and novel therapeutic targets. Oncotarget. 2015;6(14):12234-47.
33. Latres E, Drobnjak M, Pollack D, Oliva MR, Ramos M, Karpeh M, et al. Chromosome 17 abnormalities and TP53 mutations in adult soft tissue sarcomas. Am J Pathol. 1994;145(2):345-55.
34. Long Y, Tsai WB, Chang JT, Estecio M, Wangpaichitr M, Savaraj N, et al. Cisplatin-induced synthetic lethality to arginine-starvation therapy by transcriptional suppression of ASS1 is regulated by DEC1, HIF-1alpha, and c-Myc transcription network and is independent of ASS1 promoter DNA methylation. Oncotarget. 2016.
35. Phillips MM, Sheaff MT, Szlosarek PW. Targeting arginine-dependent cancers with arginine-degrading enzymes: opportunities and challenges. Cancer Res Treat. 2013;45(4):251-62.
36. Syed N, Langer J, Janczar K, Singh P, Lo Nigro C, Lattanzio L, et al. Epigenetic status of argininosuccinate synthetase and argininosuccinate lyase modulates autophagy and cell death in glioblastoma. Cell Death Dis. 2013;4:e458.
37. Delage B, Luong P, Maharaj L, O'Riain C, Syed N, Crook T, et al. Promoter methylation of argininosuccinate synthetase-1 sensitises lymphomas to arginine deiminase treatment, autophagy and caspase-dependent apoptosis. Cell death & disease. 2012;3:e342.
38. Stelter L, Evans MJ, Jungbluth AA, Longo VA, Zanzonico P, Ritter G, et al. Imaging of tumor vascularization using fluorescence molecular tomography to monitor arginine deiminase treatment in melanoma. Mol Imaging. 2013;12(1):67-73.
39. Szlosarek PW, Luong P, Phillips MM, Baccarini M, Stephen E, Szyszko T, et al. Metabolic response to pegylated arginine deiminase in mesothelioma with promoter methylation of argininosuccinate synthetase. Journal of clinical oncology : official journal of the American Society of Clinical Oncology. 2013;31(7):e111-3.
40. Stelter L, Evans MJ, Jungbluth AA, Zanzonico P, Ritter G, Ku T, et al. Novel mechanistic insights into arginine deiminase pharmacology suggest 18F-FDG is not suitable to evaluate clinical response in melanoma. J Nucl Med. 2012;53(2):281-6.
41. Ott PA, Carvajal RD, Pandit-Taskar N, Jungbluth AA, Hoffman EW, Wu BW, et al. Phase I/II study of pegylated arginine deiminase (ADI-PEG 20) in patients with advanced melanoma. Invest New Drugs. 2013;31(2):425-34.